Appl. Phys. A 78, 1197–1199 (2004)
DOI: 10.1007/s00339-003-2192-7

Applied Physics A
Materials Science & Processing

Y. LIN[1,2,✉]
F.Q. SUN[1]
X.Y. YUAN[1]
B.Y. GENG[1]
L.D. ZHANG[1]

Sol–gel electrophoretic deposition and optical properties of Fe_2O_3 nanowire arrays

[1] Institute of Solid State Physics, Chinese Academy of Science, P.O. Box 1129, Hefei 230031, P.R. China
[2] College of Material Science and Engineering, Huaqiao University, Quanzhou 362011, P.R. China

Received: 14 January 2003/Accepted: 25 March 2003
Published online: 25 July 2003 • © Springer-Verlag 2003

ABSTRACT Ordered Fe_2O_3 nanowire arrays embedded in anodic alumina membranes have been fabricated by Sol–gel electrophoretic deposition. After annealing at 600 °C, the Fe_2O_3 nanowire arrays were characterized using scanning electron microscopy (SEM), transmission electron microscopy (TEM), selected-area electron diffraction (SAED) and X-ray diffraction (XRD). SEM and TEM images show that these nanowires are dense, continuous and arranged roughly parallel to one another. XRD and SAED analysis together indicate that these Fe_2O_3 nanowires crystallize with a polycrystalline corundum structure. The optical absorption band edge of Fe_2O_3 nanowire arrays exhibits a blue shift with respect of that of the bulk Fe_2O_3 owing to the quantum size effect.

PACS 78.67.Lt; 81.05.Je; 81.07.Vb

1 Introduction

In recent years, there has been increasing interest in quasi-one-dimensional nanostructured materials because of their numerous potential applications in various areas, such as material sciences, electronics, optics, magnetics and energy storage. In the last decade, anodic alumina membranes (AAMs) have received considerable attention in synthetic nanostructured materials due to their several unique structural properties, such as controllable pore diameter, extremely narrow size distribution for the pore diameter and the pore interval, ideally cylindrical shape of the pores and good mechanical and thermal stability. They have been extensively used to fabricate nanometer-size fibrils, rods, wires and tubules of metals, semiconductors, carbons and other solid materials. Electro-chemical deposition, electroless deposition, Sol–gel deposition, chemical vapor deposition, chemical polymerization and Sol–gel electrophoretic deposition have been employed as major template-synthesis methods [1–8].

Iron- and iron-oxide-based nanomaterials have potential applications in reading and writing technologies on magnetic media [9], in catalysis [10], in magneto-optical devices [11] and particularly as superparamagnets [12]. These materials are often prepared as nanocomposites to avoid the tendency of nanoparticles to aggregate. Several attempts have been made to disperse these materials in a variety of matrix materials, such as silica [13], porous glass [14] and polymer [15]. Recently, Fe_2O_3 fibers and nanorods have been produced [16–18]. However, to the best of our knowledge, there have been no reports on the fabrication and optical properties of Fe_2O_3 nanowire arrays embedded in ordered AAMs. sol–gel electrophoretic deposition is an effective method for the fabrication of Fe_2O_3 nanowire arrays via the assistance of an AAM. This method allows combination of the advantages of the sol–gel process, namely a lower processing temperature and molecular level chemical composition homogeneity, with the advantages of electrophoretic deposition, such as fast and controlled kinetics. In this letter, we report the template-based growth of Fe_2O_3 nanowire arrays by Sol–gel electrophoretic deposition. Their optical features were also investigated.

2 Experimental

The AAM was prepared by a two-step anodization process as described previously [19, 20]. Briefly, a high-purity (99.99%) aluminum plate was annealed in vacuum at 500 °C for 3 h and degreased in acetone. The Al plate was anodized in 0.3 M oxalic acid solution under a constant voltage of 40 V for 6 h. The alumina formed was then removed with a mixture of phosphoric acid and chromic acid, and the Al sheet was anodized again under the same conditions for 12 h as mentioned above. After the second anodization, the remaining aluminum was removed in a saturated $HgCl_2$ solution. A subsequent etching treatment was carried out in a 6 wt % phosphoric acid at 30 °C to remove the barrier layer on the bottom side of the AAM. A gold layer was sputter deposited on one side of the through holes of the AAM template, to provide a conductive contact.

Fe_2O_3 colloidal suspensions for electrophoretic deposition were prepared using the same procedure as reported in [21]. Briefly, iron(III) nitrate was dissolved in 2-methoxyethanol solution ($C_6H_8O_2$). A small amount of nitric acid or ammonium hydroxide was added to the sol to adjust the pH to 2–3 and the sol was stirred for 2 h at 60 °C. The Fe_2O_3 sol thus formed was rather stable for several weeks at room temperature. For electrophoretic deposition, a platinum sheet was used as the anode, and an AAM with an Au substrate attached

✉ Fax: +86-551/5591-434, E-mail: linyuyrr@nfrn-mail.org.uk

to a Cu foil was used as the cathode. A potential of 5 V is applied between the electrodes. After electrophoretic deposition, the sample was annealed at 600 °C for 24 h in order to crystallize the Fe_2O_3 nanowires.

The sample was characterized by scanning electron microscopy (SEM, JEOL JSM-6300), transmission electron microscopy (TEM, JEM 200CX), X-ray diffraction (XRD, Philips PW 1710 with Cu K_α radiation) and UV-VIS absorption spectroscopy (Cary 5E spectrophotometer). For SEM observation, a piece of AAM with an ordered Fe_2O_3 nanowire array sample was eroded by an aqueous solution of 5 wt % NaOH for 20 min in order to remove the upper part of the AAM of the sample and then washed with distilled water several times. The sample for TEM was treated by 5 wt % NaOH solution for 40 min and then ultrasonically dispersed in ethanol.

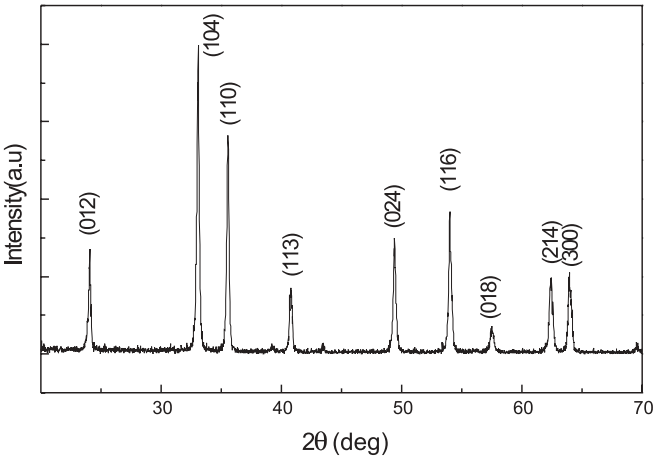

FIGURE 3 The XRD spectrum of the fabricated Fe_2O_3 nanowires

3 Results and discussion

Figure 1 shows a typical top-view SEM image of Fe_2O_3 nanowire arrays grown in the AAM template with 60-nm-diameter pores by sol–gel electrophoresis and annealed at 600 °C for 24 h. It can be seen that the nanowires are continuous and are arranged roughly parallel to one another.

The individual Fe_2O_3 nanowires were characterized by TEM after the AAM template had been thoroughly dissolved.

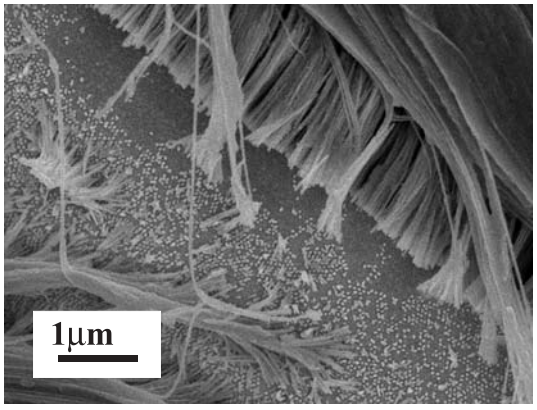

FIGURE 1 A typical SEM image of the fabricated Fe_2O_3 nanowires

High-magnification TEM images (Fig. 2a and b) showed that the Fe_2O_3 nanowires were dense and continuous. The diameter of the Fe_2O_3 nanowires is about 50 nm, which is less than the pore size of the template used. This would be well explained by the volume shrinkage due to densification during the heat treatment.

The crystalline structures of the individual Fe_2O_3 nanowires were investigated by selected-area electron diffraction (SAED) experiments. Lots of individual Fe_2O_3 nanowires were characterized and we always observed diffraction rings (Fig. 2c), indicating that the Fe_2O_3 nanowires were polycrystalline with corundum structure (α-Fe_2O_3).

Figure 3 shows the X-ray-diffraction spectrum of the Fe_2O_3 nanowire arrays. The peak positions and their relative intensities are consistent with the standard powder diffraction patterns of (α-Fe_2O_3), indicating that there is no preferred orientation and that the Fe_2O_3 nanowires are polycrystalline with corundum structure, which are in agreement with the result of SAED.

Optical absorption spectra were obtained on a Cary-5E spectrophotometer at room temperature. Figure 4 shows the optical absorption spectra of the blank AAM and the Fe_2O_3/AAM assembly system annealed at 600 °C. Two important results are evident in Fig. 4. First, the spectrum of the annealed Fe_2O_3/AAM assembly system is quite differ-

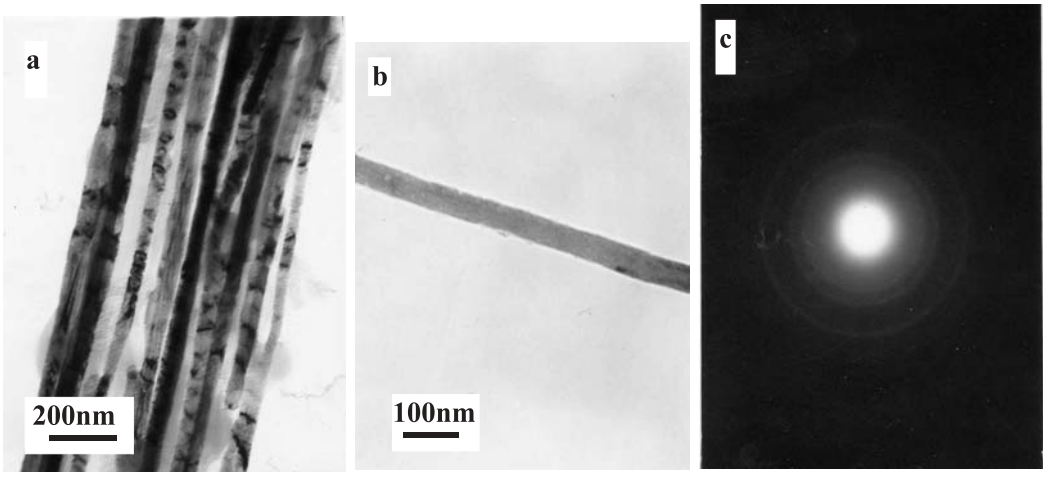

FIGURE 2 **a** A typical TEM image of several Fe_2O_3 nanowires. **b** A typical morphology of one of the Fe_2O_3 nanowires. **c** The SAED pattern taken from it

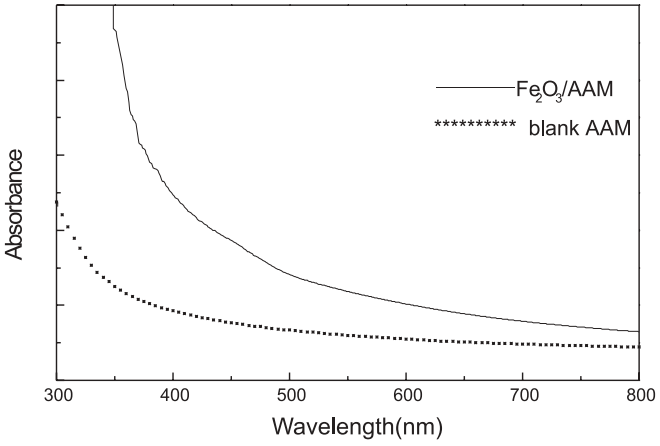

FIGURE 4 Optical absorption spectra of the Fe_2O_3 nanowire arrays in an AAM

ent from that of the blank AAM, and we do not observe the exciton absorption peaks observed in some semiconductor nanocrystal systems [22]. The second important feature is that the absorption edge of Fe_2O_3/AAM manifests itself as a strong increase of the absorption around 420 nm (2.95 eV). There are many reports concerned with quantum size effects in low-dimensional semiconductor systems. It is well known that the semiconductor nanoparticle energy gap increases with decrease of the grain size, which leads to a blue shift of the optical absorption edge, and this has been observed in many semiconductor nanoparticle systems [23–26]. Here, compared to the reported value of bulk Fe_2O_3 (2.2 eV) [27], the optical absorption band edge of the Fe_2O_3 nanowires embedded in AAM exhibits a marked blue shift with respect to that of the bulk Fe_2O_3. The blue shift could also be attributed to the quantum size effect, which leads to the broadening of the optical absorption edge.

4 Conclusions

Ordered polycrystalline α-Fe_2O_3 nanowire arrays embedded in an AAM were prepared by using sol–gel electrophoretic deposition. The individual Fe_2O_3 nanowires (diameter $\sim$50 nm) were dense and continuous. A blue shift of the optical band edge of the Fe_2O_3/AAM assembly system was observed and was mainly attributed to the quantum size effect. This Fe_2O_3/AAM assembly system can be used in magnetic, optical and gas-sensitive devices.

ACKNOWLEDGEMENTS This work was supported by the Ministry of Science and Technology of China (Grant No. G1999064501).

REFERENCES

1 G.S. Cheng, L.D. Zhang, Y. Zhu, G.T. Fei, L. Li, C.M. Mo, Y.Q. Mao: Appl. Phys. Lett. **75**, 2455 (1999)
2 J.S. Sun, J.S. Lee: Appl. Phys. Lett. **75**, 2047 (1999)
3 C.R. Martin: Science **266**, 1961 (1994)
4 A. Huczko: Appl. Phys. A **70**, 365 (2000)
5 G. Schmid: J. Mater. Chem. **12**, 1231 (2002)
6 B.B. Lakshmi, C.J. Patrissi, C.R. Martin: Chem. Mater. **9**, 857 (1997)
7 S.J. Limmer, S. Seraji, M.J. Fobress, Y. Wu, T.P. Chou, C. Nguyen, G.Z. Cao: Adv. Mater. **13**, 1231 (2002)
8 Y.C. Wang, I.C. Leu, M.H. Hon: J. Mater. Chem. **12**, 2439 (2002)
9 L. Gunther: Phys. World **2**, 28 (1990)
10 M.A. Keane: J. Catal. **166**, 347 (1997)
11 K. Dagani: Science **254**, 1300 (1991)
12 J. Kvassilion, V. Mehrotra, M.W. Russel, E.P. Giannelis, R.D. Shull, R.F. Ziolo: J. Appl. Phys. **73**, 5109 (1993)
13 G. Ennas, A. Musinu, G. Piccaluga, D. Zedda, D. Gatteschi, C. Sangregorio, J.L. Stanger, G. Concas, G. Spano: Chem. Mater. **10**, 495 (1998)
14 M.F. Borelli, D.L. Morse, J.W.H. Schreurs: J. Appl. Phys. **54**, 3344 (1983)
15 R.F. Ziolo, E.P. Giannelis, B.A. Weinstein, M.P. O'Horo, B.N. Ganguly, V. Mechrotra, M.W. Russel, D.R. Huffman: Science **257**, 219 (1992)
16 L. Vayssieres, N. Beermann, S. Lindquist, A. Hagfeldt: Chem. Mater. **13**, 233 (2001)
17 R.V. Kumar, Y. Koltypin, X.N. Xu, Y. Yeshurun, A. Gedanken, I. Felner: J. Appl. Phys. **89**, 6324 (2001)
18 C.R. Gong, D.R. Chen, X.L. Jiao, Q.L. Wang: J. Mater. Chem. **12**, 1844 (2002)
19 H. Masuda, K. Fukuda: Science **268**, 1446 (1995)
20 H. Masuda, M. Staoh: Jpn. J. Appl. Phys. Part 2 **35**, L126 (1996)
21 X.S. Niu, H. Xu: Chin. J. Appl. Chem. **17**, 611 (2000) [in Chinese]
22 N. Chestnoy, R. Hull, L.E. Brus: J. Chem. Phys. **85**, 2237 (1986)
23 T. Abe, Y. Tachibana, T. Uematsu, M. Iwamoto: J. Chem. Soc. Chem. Commun. 1617 (1995)
24 A.D. Yoffe: Adv. Phys. **42**, 173 (1993)
25 C. Cormann, D.W. Bahnemann, M.R. Hoffmann: J. Phys. Chem. **92**, 5196 (1988)
26 F. Bentivegna, M. Nyvlt, J. Ferre, J.P. Jamet, A. Brun, S. Visnovsky, R. Urban: J. Appl. Phys. **85**, 2270 (1999)
27 H. Miyoshi, H. Yoneyama: J. Chem. Soc. Faraday Trans. **85**, 1873 (1989)